THE JOURNAL OF PHYSICAL CHEMISTRY A

 VOLUME 105, NUMBER 38, SEPTEMBER 27, 2001

ARTICLES

Time-Resolved Raman Studies of Photoionization of Aromatic Compounds in Polar Solvents: Picosecond Relaxation Dynamics of Aromatic Cation Radicals

Takakazu Nakabayashi,[†] Satoshi Kamo,[†,‡] Hirochika Sakuragi,[‡] and Nobuyuki Nishi*[,†]

Institute for Molecular Science, Myodaiji, Okazaki 444-8585, Japan, and Department of Chemistry, University of Tsukuba, Tennodai, Tsukuba, 305-8571, Japan

Received: March 16, 2001; In Final Form: June 27, 2001

Picosecond time-resolved Raman spectroscopy has been used to study the ultrafast relaxation dynamics of aromatic cation radicals following two-photon ionization. In acetonitrile, integrated Raman intensities due to the cation radicals rise in tens of picoseconds, and reach their maxima at a delay time of 40−60 ps from the pump pulse. Such a slow-rise component is observed in all the cation radicals treated (biphenyl, *trans*-stilbene and naphthalene), suggesting that the picosecond relaxation process increasing the cation Raman intensities occurs after the photoionization of aromatic molecules. In weak polar solvents such as ethyl acetate, on the other hand, only an instrumental-limited rise (<5 ps) is observed. The rise time of the cation Raman intensity does not correlate with the dielectric relaxation time but depends on the polarity of the solvent. This result indicates that the picosecond relaxation process is not controlled by the dielectric solvent relaxation alone. The positional changes and the band narrowings of the cation Raman bands occur on a 10−20 ps time scale. These are associated with intermolecular vibrational relaxation of the cation radical toward a thermal equilibrium with solvents. The time scale of the intermolecular vibrational relaxation is the same as that of the rise component of the cation Raman intensity. From these observations, it is suggested that the thermal excitation of the solvent shell disturbs the solvation structure of the cation radical, which causes the observed picosecond change in the cation Raman intensity.

1. Introduction

Photoionization of aromatic compounds in condensed phase has been studied extensively in view of its importance in many areas of chemistry and physics.[1−4] Progress has been made in understanding the factors governing the quantum yield for ionization, the dynamics of ion solvation and the reactivity of generated species. Photoionization process in solution phase may be roughly classified into two groups according to the solvent examined: nonpolar and polar media. In nonpolar solvents where there is only weak solute−solvent interactions, the dynamics following ionization has been considered to be described as the classical diffusion of the ions in a Coulombic field; the solvent is treated only as a continuous medium.[1−11] Immediately after photoionization, a photoelectron ejected from a molecule scatters on a continuous medium and becomes thermalized with a certain distance from its parent cation. The resultant cation−electron distance depends on the initial translational energy of the photoelectron and is, in most cases, much smaller than the average Onsager radius at which the Coulomb binding energy of the ion pair is equal to the thermal energy kT.[12] Thus the majority of the electrons geminately recombine

* Corresponding author: Professor Nobuyuki Nishi, Department of Electronic Structure, Institute for Molecular Science, Myodaiji, Okazaki 444−8585, Japan. Fax: +81-564-54-2254. E-mail: nishi@ims.ac.jp.
[†] Institute for Molecular Science.
[‡] University of Tsukuba.

10.1021/jp0110105 CCC: $20.00
Published on Web 08/31/2001

with their parent cations within several picoseconds at room temperature, while the remainder escape and homogeneously recombine with other cations more slowly. This applies even in pulse radiolysis experiments where the electron can be ejected with a substantial amount of energy.[2,3]

In polar solvents, on the other hand, solvent dynamics of the reorganization around an ionized molecule should be considered because of strong solute−solvent interactions.[1,13−21] In the same way as in the case of nonpolar media, an ionizing event in polar solvents can be characterized by the production of an electron−cation ion pair. Then surrounding solvent molecules respond to the instantaneous charge creation and show reorganization in the time range of femto- to picoseconds.[14,18−20] Vibrational relaxation as well as structural relaxation can also occur in this time range, resulting in the generation of the solvated-free ions with lifetimes longer than nanoseconds. If the initial cation−electron distance is shorter than the Onsager radius, then geminate recombination should compete with the formation of the solvated free ions. However, since there have been very few ultrafast studies on the photoionization of large molecules in polar media,[14] all the dynamics remain unresolved despite their importance in photochemistry. Time-resolved electronic absorption spectroscopy has been adopted most frequently as a tool for studying ultrafast dynamics of nonfluorescent molecules;[1−4,6−11,13−16] however, in many cases, the overlapping among the broad absorption bands arising from the ions and the parent aromatic molecule in electronically excited states makes it difficult to study the relaxation dynamics of the ions following the photoionization.

Both spontaneous and coherent time-resolved Raman spectroscopic techniques are well recognized as powerful methods for studying the structure and dynamics of short-lived species.[22] The vibrationally resolved spectra also have the potential for distinguishing coexisting transient species from each other even in solvents. Nanosecond time-resolved Raman measurements have therefore been applied to the study of photoionization and photoinduced electron-transfer reactions of conjugated systems in solvents by several groups.[17,21,23−25] Kamisuki et al. have studied photoionization of diphenylbutadiene and diphenylhexatriene in various polar solvents by nanosecond coherent anti-Stokes Raman scattering (CARS) spectroscopy.[17] They suggested the presence of competition between the biphotonic ionization and the solvent-assisted monophotonic ionization in polar solvents under the excitation at 337 nm. Sasaki and Hamaguchi have made use of the nanosecond time-resolved Raman technique to the study of monophotonic ionization of biphenyl in alcohols.[21] They estimated the formation rate of the cation radical from the first excited singlet (S_1) state not to be greater than 10^{-7} s^{-1}. Vauthey et al. have studied the 1,2,4-trimethoxybenzene/9,10-anthraquinone system by nanosecond time-resolved Raman spectroscopy and observed the structural change in the cation radical of 1,2,4-trimethoxybenzene, corresponding to the separation of the geminate ion pair into the free ions.[23,24] Photoinduced electron-transfer reactions between *trans*-stilbene and aromatic cyanocompounds in acetonitrile have also been analyzed by nanosecond Raman spectroscopy.[25]

Oberlé et al. have made use of the time-resolved CARS technique and, to our knowledge, have first reported photoionization dynamics of conjugated systems in polar solvents with a time resolution of several picoseconds.[26] The CARS intensity arising from the cation radical of 1,4-diphenylbutadiene was seen to rise with a time constant of 10−20 ps. This slow rise was attributed to the formation and stabilization dynamics of the cation radical. Incident excitation-laser power dependence suggested that the formation process of the observed cation radical was mainly monophotonic under the excitation at 300 nm. For this reason, 1,4-diphenylbutadiene in the S_1 state can be considered to be a precursor of its cation radical. If the cation radical is generated via the S_1 state, the lifetime of the S_1 state should not be longer than the formation time of the cation radical. However, the lifetime of 1,4-diphenylbutadiene in the S_1 state estimated by time-resolved absorption spectroscopy was over twice as long as the rise time of the cation CARS intensity.[26] Therefore, careful consideration may be needed to clarify the origin of the picosecond rise component of the cation Raman intensity in polar solvents.

To our best knowledge, no one has reported picosecond time-resolved Raman spectra of aromatic cation radicals except the CARS spectra mentioned above. This is primarily due to the difficulty in obtaining the wavelength tunability of picosecond pulses applicable to time-resolved Raman spectroscopy, in which the pump wavelength should be tuned for the effective ionization of the target molecule and the probe wavelength should be in resonance with the cation absorption. In the present study, we have constructed a two-color independently tunable Raman spectrometer with a time resolution of several picoseconds, and have observed picosecond time-resolved Raman spectra of aromatic cation radicals (biphenyl, *trans*-stilbene and naphthalene) in several polar solvents. From measurements of excitation-laser power, solvent, probe-wavelength, and sample dependencies, we discuss ultrafast solvation and vibrational relaxation dynamics of the aromatic cation radicals following the photoionization.

2. Experimental Section

Output pulses from a femtoecond mode-locked Ti:sapphire laser (Spectra Physics, Tsunami 3941, wavelength 790 nm, repetition rate 80 MHz, average power 0.9 W, pulse duration 250 fs) were put into a picosecond regenerative amplifier (Quantronix, Taitan) pumped by a Q-switched intracavity frequency-doubled Nd:YLF laser (Quantronix, 527DP−H, 527 nm, 1 kHz, 15 W, 150 ns). Amplified pulses with ∼4 ps pulse duration, 790 nm wavelength, and 2.8 μJ pulse energy were obtained at a repetition rate of 1 kHz. A half of the amplified output was frequency doubled to excite an optical parametric amplifier (OPA) system (Light Conversion, TOPAS 4/400). By using second harmonic and sum-frequency mixing techniques, we obtained approximately a continuous tuning of light between 190 and 2700 nm with keeping microjoule pulse energy. The remainder of the amplified output was used to excite the other OPA system (Light Conversion, TOPAS 4/800). Light pulses with microjoule pulse energy in the region between 230 and 11200 nm were obtained with second harmonic and sum- and difference-mixing techniques. The output from the former OPA system was used as the pump beam for ionizing aromatic molecules, and the output from the latter one was used as the probe beam for resonance Raman observation.

After passing through fixed (for the pump beam) and variable (for the probe beam) optical delay lines, the pump and probe beams were superimposed by a dichroic mirror, and focused onto the sample solution with an $f = 70$ mm lens. The focused area was $\sim 2 \times 10^{-3}$ cm^2. The sample solution was flowed through a squeezed stainless steel nozzle to form a thin (∼0.3 mm) liquid jet. The average pump- and probe-pulse energies were 3−4 μJ and 0.5−0.8 μJ, respectively. The electric vectors of the pump and probe fields were set parallel to each other in the spectra reported here. Measurements with the pump and probe electric vectors set perpendicular to each other were also

performed. From the calculations of the isotropic components of the polarized scattering intensities,[27,28] the temporal behavior was confirmed not to be affected by the polarization between the pump and probe pulses within the experimental accuracy. The instrumental response function was determined by a sum-frequency mixing technique in a 0.5 mm BBO crystal and temporal rises of the excited-state absorption intensities of the sample molecules. It was estimated to be a Gaussian function with a full width at half-maximum of 4.3 ps.

The 90°-scattered Raman signal was collected and dispersed by a single spectrograph (JOBIN YVON-SPEX, 500MS), and detected by a CCD detector (Princeton Instruments, LN/CCD-1340PB, 1340 × 400 pixels). The unshifted scattered light was rejected with a holographic notch filter (Kaiser Optical Systems) or a color glass filter (SIGMA KOKI) placed in front of the entrance slit of the spectrograph. The spectral slit width was ~10 cm^{-1}. In a series of measurements, the order of the delay time was set to be random to minimize effects of long-term drifts of the laser system on the observed kinetics. At each delay time the exposure time was 200 s. The transient Raman spectra were taken by the average of the data for 9−40 cycles. The pump-only and probe-only spectra were subtracted from the pump−probe spectra, providing the spectra of photoproducts reported here. Effects of reabsorption due to the transient species at each delay time were reduced by the normalization of the data to the intensity changes in the solvent Raman bands. Multiple photoionization of solvents was confirmed to have no effect on the time-resolved Raman spectra from measurements of solutions without solutes. Emission lines from a neon lamp were used to determine the wavelengths of the laser beams and to calibrate the Raman spectra. Sample molecules and solvents (Wako Pure Chemical Industries, special reagent grade) were used as received. The concentration of the sample solution was 1×10^{-3} mol dm^{-3}. All experiments were carried out at room temperature (293 K).

3. Results

3.1. Incident Laser Power Dependencies of Transient Raman Spectra. As mentioned earlier, monophotonic as well as biphotonic ionization has been considered to occur in the ultraviolet photoexcitation of some conjugate systems even in the picosecond time range.[26] To examine whether the observed cation radicals are formed via one-photon or two-photon absorption, therefore, we have first observed picosecond time-resolved Raman spectra of the cation radicals with different magnitudes of the pump-laser power. Furthermore, the probe-laser power dependence of the time-resolved Raman spectra should also be examined. When the probe-photon density is very high, the S_1 species generated by the pump photon may be ionized by absorbing the visible probe photon. In this case, the Raman intensities arising from the cation radical should exhibit a quadratic dependence on the probe-laser power.

Figure 1, parts A and B, show the pump- and probe-laser power dependencies of the transient resonance Raman spectra of biphenyl at 120 ps delay time, respectively. Arrows indicate Raman bands arising from the cation radical of biphenyl and the other Raman bands are ascribed to biphenyl in the S_1 state.[21,29,30] Plots of the transient Raman intensities against the pump-pulse energy at the sample are also shown in Figure 1C. As shown in Figure 1, parts A and C, the Raman intensities due to the S_1 transient are almost linearly dependent on the pump-pulse energy as expected, while those due to the cation radical exhibit almost the quadratic dependence on the pump-pulse energy. As for the probe-laser power dependence in Figure 1B, both the Raman intensities due to biphenyl in the S_1 state and its cation radical are approximately proportional to the probe−pulse energy when the pulse energy is less than ~1 μJ. As the probe−pulse energy is increased beyond this value, both the Raman intensities begin to show sublinear dependencies on the probe−pulse energy, which may be partly due to the depletion of the transient species by the photoexcitation. However, in any energy range, a quadratic (or higher-order) dependence of the transient Raman intensity on the probe−pulse energy is not observed. It is noted in Figure 1 that the band shapes and the peak positions of all the Raman bands are hardly affected by the incident pulse energy. The results for *trans*-stilbene and naphthalene also show the same behavior. From the results described above, it is concluded that the cation radicals observed in the present study are formed via the two-photon absorption of the ultraviolet pump radiation. The one-photon ionization has only minor effects, if any, on the observed Raman spectra of the cation radicals.

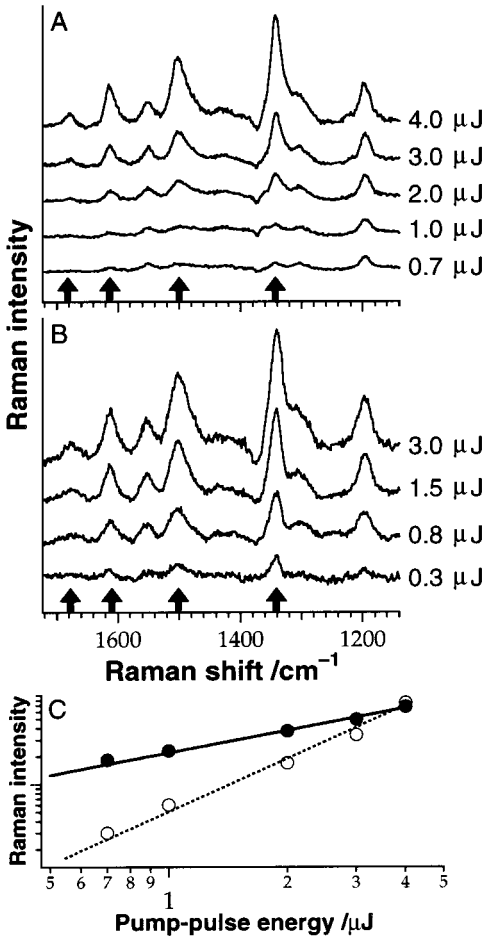

Figure 1. Pump-laser power (A) and probe-laser power (B) dependencies of transient Raman spectra of biphenyl in acetonitrile at 120 ps delay time. The pump-pulse energy (A) or the probe-pulse energy (B) is given on the right side of each spectrum. Arrows indicate Raman bands arising from the cation radical of biphenyl and the other bands are due to biphenyl in the S_1 state. The Raman bands of acetonitrile are subtracted. Pump, 262 nm; probe, 633 nm. (C) Plots of the Raman intensities of the cation radical of biphenyl at 1614 cm^{-1} (open circles) and of biphenyl in the S_1 state at 1195 cm^{-1} (filled circles) in acetonitrile at 120 ps delay time against the pump-pulse energy on a log−log scale.

3.2. Solvent Dependence of Time-Resolved Raman Intensities of Biphenyl. To examine the solvent dependence of the Raman spectra of biphenyl, we have used the same wavelengths and energies of the incident pump (262 nm, 3 μJ) and probe

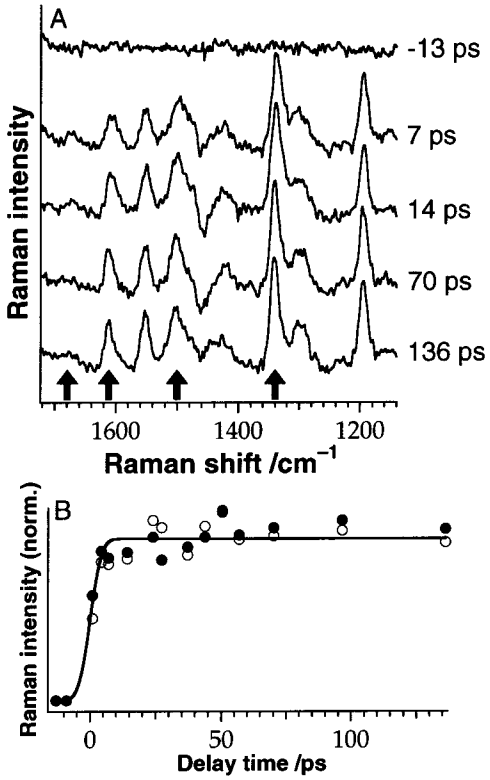

Figure 2. (A) Picosecond time-resolved Raman spectra of biphenyl in ethyl acetate. Arrows indicate Raman bands arising from the cation radical of biphenyl and the other bands are due to biphenyl in the S_1 state. The delay time is given on the right of each spectrum. Pump, 262 nm; probe, 633 nm. (B) Plots of the normalized Raman intensities of the cation radical of biphenyl at 1341 cm^{-1} (open circles) and of biphenyl in the S_1 state at 1195 cm^{-1} (filled circles) in ethyl acetate against the delay time. The solid curve represents the fit to the data by the convolution of the instrumental function with a nanosecond decay exponential function.

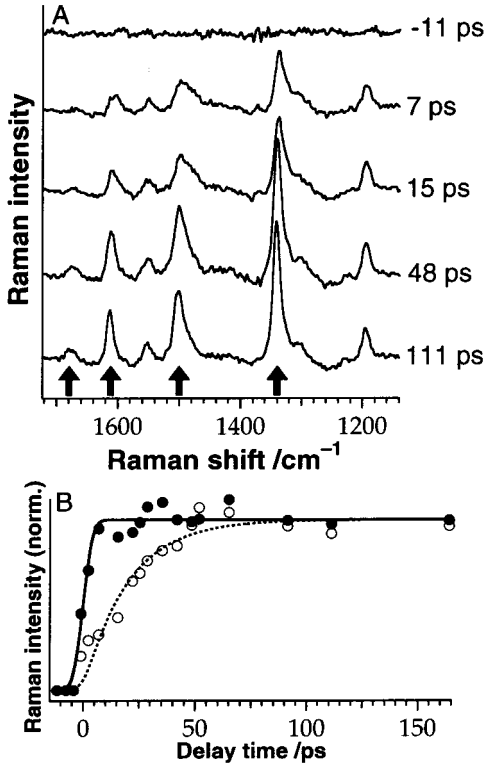

Figure 3. (A) Picosecond time-resolved Raman spectra of biphenyl in acetonitrile. Arrows indicate Raman bands arising from the cation radical of biphenyl and the other bands are due to biphenyl in the S_1 state. The delay time is given on the right of each spectrum. Pump, 262 nm; probe, 633 nm. (B) Plots of the normalized Raman intensities of the cation radical of biphenyl at 1341 cm^{-1} (open circles) and of biphenyl in the S_1 state at 1195 cm^{-1} (filled circles) in acetonitrile against the delay time. The solid curve represents the fit to the S_1 data by the convolution of the instrumental function with a nanosecond exponential decay function. The dotted curve represents the best fit to the cation data by the convolution of the instrumental function with two exponential functions (a picosecond rise and a nanosecond decay). The time constant of the rise component is 20 ps.

(633 nm, 0.8 μJ) laser pulses. The picosecond time-resolved resonance Raman spectra of biphenyl in ethyl acetate are shown in Figure 2A, in which arrows indicate Raman bands arising from the cation radical of biphenyl and the other Raman bands are due to biphenyl in the S_1 state.[21,29,30] Raman bands of the solvent are completely subtracted in these spectra. The Raman bands due to biphenyl in the S_1 state and its cation radical can be simultaneously observed since the probe wavelength of 630 nm is in pre-resonance with both the S_1 and the cation absorption bands at 660 and 680 nm, respectively.[21] As for the cation radical, the assignments of the observed Raman bands have been performed.[29,30] The prominent Raman band at ~1341 cm^{-1} is ascribed to the inter-ring C−C stretching mode. The relatively broad Raman band at ~1501 cm^{-1} is due to a mode with a major contribution from the ring stretch and the inter-ring C−C stretch. Another band at ~1614 cm^{-1} is also assigned to a mode consisting of the ring stretch and the inter-ring C−C stretch. The 1674 cm^{-1} band is assigned to a combination band due to the inter-ring C−C stretching mode (~1341 cm^{-1}) and the ring deformation mode (~334 cm^{-1}). As far as we know, the assignments of the observed Raman bands of biphenyl in the S_1 state have not been performed. Only exception is that the S_1 Raman band at ~1551 cm^{-1} is reported to correspond to the cation band at ~1614 cm^{-1}.[29]

The time developments of the integrated intensities of the transient Raman bands of biphenyl in ethyl acetate are shown in Figure 2B. No mode-specific changes are observed in both the Raman intensities of biphenyl in the S_1 state and its cation radical within our experimental uncertainty. The S_1 and the cation Raman intensities exhibit almost the same temporal behavior. Both the time-resolved curves rise within the experimental temporal resolution (<5 ps), and then remain almost unchanged for delay times >10 ps. This result is consistent with the expectation that both the S_1 and the cation transients are generated immediately after one-photon and two-photon excitation, respectively, and have lifetimes longer than 1 ns.[21] No decay component due to the geminate recombination is observed in the cation Raman intensities.

Figure 3A shows the picosecond time-resolved Raman spectra of biphenyl in acetonitrile. Plots of the integrated Raman intensities against the delay time are also shown in Figure 3B. Apparently, the cation Raman intensity in acetonitrile shows the temporal profile different from that in ethyl acetate. In acetonitrile, the Raman intensities due to the cation radical of biphenyl rise in tens of picoseconds, and reach their maxima at ~50 ps. On the other hand, the Raman intensities arising from biphenyl in the S_1 state show instrumental-limited rises (<5 ps), indicating that the temporal profile of the S_1 Raman intensity is the same as those of the S_1 and the cation Raman intensities in ethyl acetate. The changes in the cation Raman intensities can be satisfactorily reproduced by the convolution of the instrument response function with two exponential functions (a picosecond rise and a nanosecond decay). The best-fit time constant of the rise component is 20 ps. No mode-specific

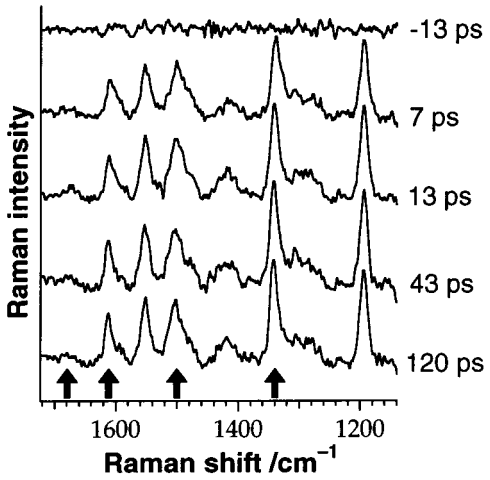

Figure 4. Picosecond time-resolved Raman spectra of biphenyl in 1-butanol. Arrows indicate Raman bands arising from the cation radical of biphenyl and the other bands are due to biphenyl in the S_1 state. The delay time is given on the right of each spectrum. Pump, 262 nm; probe, 633 nm.

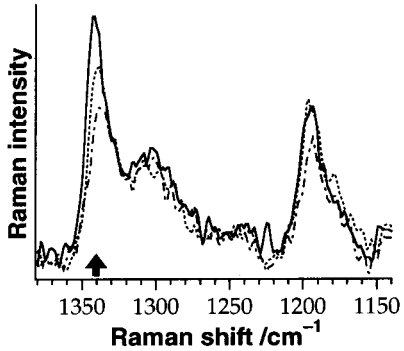

Figure 5. Picosecond time-resolved Raman spectra of biphenyl in propylene carbonate. Arrows indicate Raman bands arising from the cation radical of biphenyl and the other bands are due to biphenyl in the S_1 state. Dot−dashed trace, 5 ps; dotted trace, 13 ps; solid trace, 50 ps. Pump, 262 nm; probe, 633 nm.

changes are observed in both the S_1 and the cation Raman intensities. The peak positions of the observed cation Raman bands show little shifts with the change of the solvent from ethyl acetate to acetonitrile. It is noted that, in acetonitrile, the intensities of the cation bands relative to those of the S_1 bands are much larger than those in ethyl acetate.

The picosecond time-resolved Raman spectra of biphenyl in 1-butanol are shown in Figure 4. The viscosity of 1-butanol is reported to be 2.54 cp at 298 K, which is over five times as large as those of acetonitrile (0.37 cp) and ethyl acetate (0.43 cp).[31] Thus the slow dynamics is expected in the time-resolved spectra in 1-butanol if any orientational reorganization is responsible for the rise of the Raman signals. However, both the Raman intensities arising from biphenyl in the S_1 state and its cation radical show the instrumental-limited rises and remain almost unchanged for delay times >10 ps. Figure 5 shows the picosecond time-resolved Raman spectra of biphenyl in propylene carbonate. This solvent is known to be an aprotic and highly polar solvent like acetonitrile.[31,32] It has not been successful to obtain good quality Raman spectra in propylene carbonate because of interference by fluorescence arising from the sample as well as impurities. However, it is seen in Figure 5 that the intensity of the cation Raman band at 1341 cm^{-1} rises more slowly than that of the S_1 band at 1195 cm^{-1}. This suggests that the cation Raman intensity in propylene carbonate

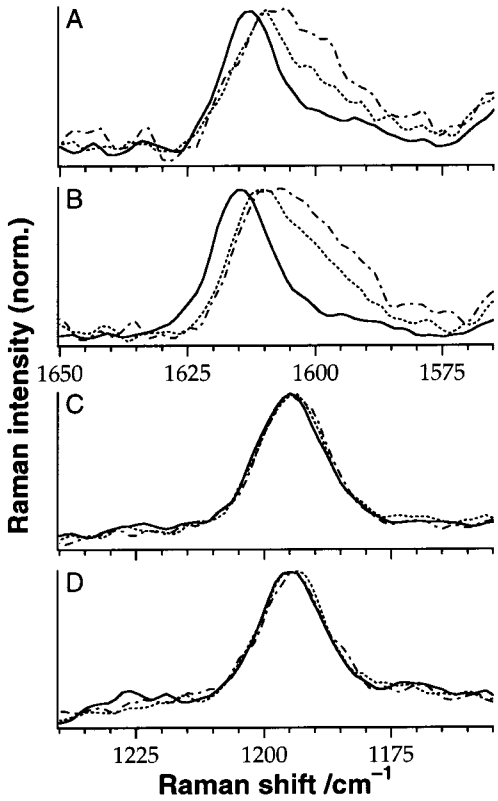

Figure 6. Time dependence of the Raman band of the cation radical of biphenyl at 1614 cm^{-1} in ethyl acetate (A) and in acetonitrile (B), and of the Raman band of biphenyl in the S_1 state at 1195 cm^{-1} in ethyl acetate (C) and in acetonitrile (D). Pump, 262 nm; probe, 633 nm. The intensity scale is normalized for the peak intensities of the respective spectra. Dot−dashed trace, 5 ps; dotted trace, 13 ps; solid trace, 50 ps. Pump, 262 nm; probe, 633 nm.

rises in tens of picoseconds. This temporal behavior is similar to the result of the cation Raman intensity in acetonitrile.

3.3. Temporal Changes in Center Wavenumbers of Transient Raman Bands of Biphenyl. As seen in Figures 2−5, peak positions of the cation Raman bands also change with the delay time, being accompanied by band narrowing. Panels A and B in Figure 6 show the temporal spectral changes of the Raman band of the cation radical of biphenyl at 1614 cm^{-1} in ethyl acetate and acetonitrile, respectively. The intensity scale is normalized for the peak intensities of the respective spectra. In contrast to the results on the Raman intensities, the temporal changes in the peak positions and the bandwidths are observed in all the solvents used in the present study. Such spectral changes are seen in all the cation Raman bands observed in Figures 2−5. Plots of the center wavenumber of the 1614 cm^{-1} band against the delay time are shown in Figure 7. To estimate the center wavenumber (ν_c), we adopt the first moment analysis, which is given by the following form:

$$\nu_c = \frac{\sum_i \nu_i I(\nu_i)}{\sum_i I(\nu_i)} \quad (1)$$

where $I(\nu_i)$ and ν_i represent the Raman intensity and the wavenumber at the pixel number of the detector i, respectively.[33] This method has the advantage that no assumption is needed for a Raman band shape.[33] The observed time profiles are satisfactorily reproduced by the convolution of the instrument

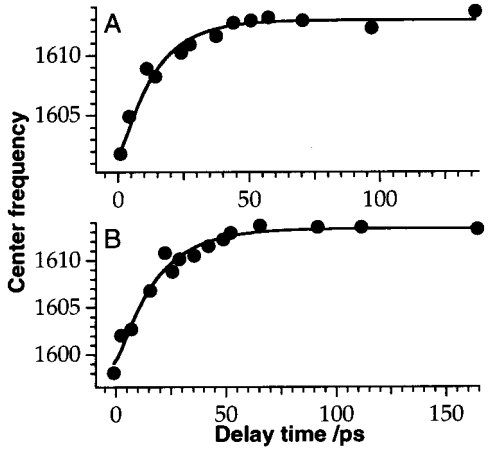

Figure 7. Temporal changes in the center wavenumber of the Raman band of the cation radical of biphenyl at 1614 cm^{-1} in ethyl acetate (A) and in acetonitrile (B). The solid curves represent the best fits to the data by the convolution of the instrumental function with a single-exponential function. The obtained time constants are 13 ps (A) and 17 ps (B).

response function with single-exponential functions, yielding time constants of 13 ps in ethyl acetate and 17 ps in acetonitrile. In acetonitrile, the time constant obtained from the center-wavelength change is similar to that obtained from the intensity change mentioned in subsection 3.2.

Panels C and D in Figure 6 show the temporal spectral changes of the Raman band of biphenyl in the S_1 state at 1195 cm^{-1} in ethyl acetate and acetonitrile, respectively. In both the solvents, no marked changes in the center wavenumbers and the bandwidths are seen in all the S_1 Raman bands in the region of 1140−1750 cm^{-1}. The S_1 Raman bands in 1-butanol and propylene carbonate also show the same behavior. Such a temporal profile is obviously different from the results on the cation Raman bands in panels A and B. It is hence concluded that the changes in the center wavenumbers and the bandwidths are observed especially in the Raman spectra of the cation radical of biphenyl, which is independent of the solvent used.

3.4. Probe-Wavelength Dependence of Time-Resolved Raman Spectra of Biphenyl. It has been reported that the cation radical of biphenyl has a strong absorption around 680 nm.[21] Thus the probe wavelength of 630 nm used in all the above figures is slightly off resonance from the absorption maximum of the cation radical. The use of the 630-nm probe light has the advantage that both the S_1 and the cation Raman bands are simultaneously observed and the time profiles of the S_1 Raman intensities can be used for checking the response functions of the measurements. However, it is important to observe the Raman spectra with the probe wavelength tuned around the absorption maximum, since there is a possibility that the slow increase in the cation Raman intensity is due to picosecond spectral changes of the absorption of the cation radical such as band narrowing.

By using the probe wavelength of 680 nm being resonance with the cation absorption maximum, we have observed the picosecond time-resolved Raman spectra of biphenyl in ethyl acetate and acetonitrile, which are shown in panels A and B in Figure 8, respectively. Because of the resonance effect, Raman bands arising from biphenyl in the S_1 state are hardly observed in this figure. In acetonitrile, the intensity of the cation band exhibits a rise as slow as tens of picoseconds, while that of the cation band in ethyl acetate rises instantaneously. Such temporal behavior is almost the same as the result obtained with the 630-nm probe light in Figures 2 and 3. Changes in the center

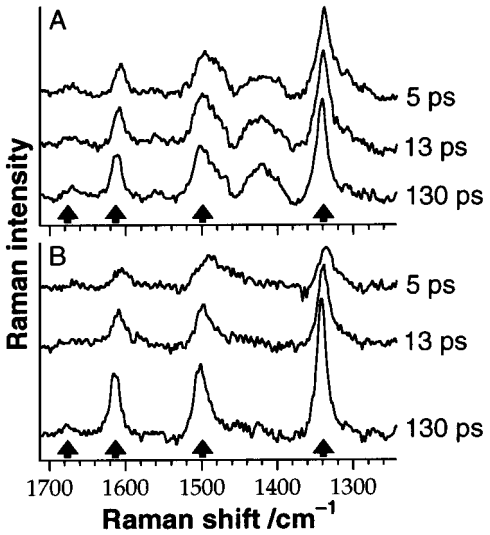

Figure 8. Picosecond time-resolved Raman spectra of biphenyl in ethyl acetate (A) and in acetonitrile (B). Arrows indicate Raman bands arising from the cation radical of biphenyl. The delay time is given on the right of each spectrum. Pump, 262 nm; probe, 680 nm.

wavenumbers and the bandwidths of the cation bands are also observed in both the solvents. These results lead us to the conclusion that the observed temporal changes in the cation Raman bands are almost independent of the probe wavelength used. A broad feature at ∼1420 cm^{-1} is seen in Figure 8A, which may be attributable to neither biphenyl in the S_1 state nor its cation radical. Although the possibility of the $T_n \rightarrow T_1$ emission has been proposed,[21] careful consideration is needed to reach a more definitive conclusion on this point.

3.5. Picosecond Time-Resolved Raman Spectra of *trans*-Stilbene and Naphthalene. Figure 9A shows the picosecond time-resolved resonance Raman spectra of *trans*-stilbene in acetonitrile. The pump and probe wavelengths are 262 and 529 nm, respectively. Three arrows indicate Raman bands due to the cation radical of *trans*-stilbene and the other Raman bands are attributed to *trans*-stilbene in the S_1 state.[34,35] Raman bands of the solvent are subtracted. The strong Raman band arising from the cation radical at ∼1605 cm^{-1} is assigned to the phenyl C═C stretching mode.[34] Figure 9B shows the time developments of the integrated intensities of the cation band at 1605 cm^{-1} and of the S_1 band at 1243 cm^{-1}. For the estimation of the cation Raman intensities, band fitting analyses for the 1560−1680 cm^{-1} region are performed with three Lorentzian functions.[36] The rise of the cation Raman intensity is slow, which is well described with a single-exponential function with a time constant of 17 ps, while the S_1 Raman intensity rises instantaneously (<5 ps) and decays with the S_1 lifetime of 40 ps.[26] The slower rise of the cation Raman intensity in acetonitrile is similar to the result of the cation Raman intensity of biphenyl in the same solvent.

Figure 10 shows the picosecond time-resolved resonance Raman spectra of naphthalene in acetonitrile. The pump and probe wavelengths are 262 and 670 nm, respectively. Only the resonance Raman bands arising from the cation radical of naphthalene are observed in this figure.[37] Fluorescence arising from the $S_1 \rightarrow S_0$ transition of naphthalene seriously interferes with the Raman measurements; however, the rises of the cation Raman intensities are as slow as ∼25 ps. We have also observed the instantaneous rises of the Raman intensities of the cation radical of naphthalene in ethyl acetate.

From these results, the slow increase in the Raman intensity in acetonitrile is found to be observed in all the aromatic cation

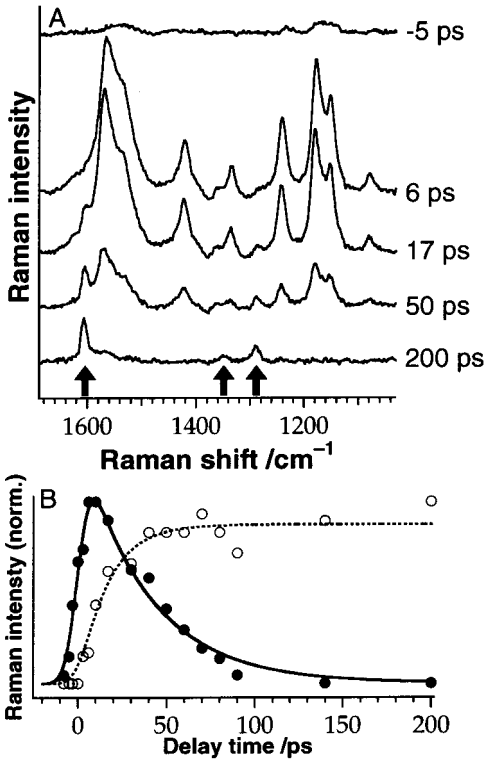

Figure 9. (A) Picosecond time-resolved Raman spectra of *trans*-stilbene in acetonitrile. Arrows indicate Raman bands arising from the cation radical of *trans*-stilbene and the other bands are due to *trans*-stilbene in the S_1 state. The delay time is given on the right of each spectrum. Pump, 262 nm; probe, 529 nm. (B) Plots of the normalized Raman intensities of the cation radical of *trans*-stilbene at 1605 cm^{-1} (open circles) and of *trans*-stilbene in the S_1 state at 1243 cm^{-1} (filled circles) in acetonitrile against the delay time. The solid curve represents the best fit to the S_1 data by the convolution of the instrumental function with a decay exponential function. The time constant of the decay component is 40 ps. The dotted curve represents the best fit to the cation data by the convolution of the instrumental function with two exponential functions (a picosecond rise and a nanosecond decay). The time constant of the rise component is 17 ps.

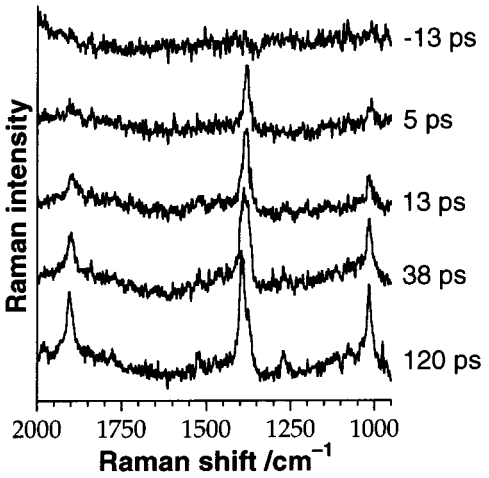

Figure 10. Picosecond time-resolved Raman spectra of naphthalene in acetonitrile. All the observed bands are due to the cation radical of naphthalene. The delay time is given on the right of each spectrum. Pump, 262 nm; probe, 670 nm.

radicals treated in the present study. Therefore, it may be now concluded that the Raman intensity due to the aromatic cation radical generally exhibits the picosecond slow rise after the photoionization in acetonitrile.

4. Discussion

4.1. Temporal Changes in Center Wavenumbers of Transient Raman Bands. Time-resolved vibrational spectroscopy provides microscopic details of the solute−solvent interactions and the structural changes occurring on photoexcitation through multiple parameters: center wavenumbers, bandwidths and intensities.[22,26,33,35,38−54] In this section, we first focus on the temporal changes in the center wavenumbers of the cation Raman bands. The slow increases in the cation Raman intensities are discussed in the next subsection.

Vibrational population relaxation process (simply called in this paper as "vibrational relaxation"), which is defined as the transition process from a vibrationally excited state to a thermodynamically favorable state, is regarded as one of the earliest molecular processes immediately after photoexcitation. In solution, vibrational relaxation is considered to proceed in roughly two steps.[55] Immediately after photoexcitation and/or nonradiative electronic transition, excess vibrational energy is considered to be localized on Franck−Condon active modes. The localized energy is distributed within the solute molecule to other vibrational modes (intramolecular vibrational relaxation). Very rapid redistribution of the excess energy creates a quasi-equilibrium among all intramolecular vibrational modes, resulting in a single, mode-independent vibrational temperature. Solute−solvent energy transfer (intermolecular vibrational relaxation) also occurs to achieve a thermal equilibrium with solvents. For medium-size to large molecules in solution, it has been thought that the typical time scale of the intramolecular relaxation is in the subpicosecond range and that of the intermolecular relaxation in tens of picoseconds.[55] Several recent experiments, however, have suggested that the intramolecular vibrational relaxation process may not be completed within a few picoseconds in some cases.[33,46,47,49,56]

For studying intermolecular vibrational relaxation in solutions, analyses of the changes in center wavenumbers and bandwidths of picosecond time-resolved Raman bands have been recognized as one of the useful method.[22,26,33,35,38−53] Iwata and Hamaguchi have analyzed the high-wavenumber shifts and the band narrowings of the picosecond time-resolved Raman bands of *trans*-stilbene in the S_1 state.[38,39] The time dependence of the peak position of the olefinic C═C stretching band was found to be a good indicator of the vibrational temperature change in the solute.[39] Mizutani et al. have shown that the time constant for the high-wavenumber shift of the (Stokes) Raman band of nickel octaethylporphyrin is close to those for the decays of the populations on the vibrationally excited levels observed as the anti-Stokes Raman intensity decays.[33] The high-wavenumber shifts and the band narrowings of the vibrational bands, which occur on a picosecond time scale, have been observed in other vibrationally hot polyatomic neutral molecules.[26,35,40−54] All the dynamics have been considered to be associated with intermolecular vibrational relaxation of hot neutral solutes toward thermal equilibria with solvents.

The high-wavenumber shifts and the band narrowings of the cation Raman bands in Figures 2−10 are similar to the results of the polyatomic neutral molecules mentioned above.[26,33,35,38−53] This spectral evolution is observed in all the solvents used, and is observed in the Raman bands of all the cation radicals treated in the present study. Since the ionization energies of the treated aromatic molecules in the gas phase are in the range of 150−162 nm,[31] the excess energy (in this case, difference between energies of the sum of the two pump photons and the ionization threshold) should be very large. Thus, immediately after the biphotonic ionization, the molecular vibrations can receive a

large amount of excess energy, generating the vibrationally excited cation radical. It can be therefore concluded that the high-wavenumber shifts and the band narrowings of the cation Raman bands are associated with the intermolecular vibrational relaxation of the cation radical toward a thermal equilibrium with solvent molecules. In the analyses of photoionization dynamics of aromatic molecules, the excess energy has sometimes been assumed to be entirely left with the ejected electron as the translational energy.[5,8] This result, however, indicates that the excess energy is left with the vibrational modes of the cation radical as well as the ejected electron. According to the Franck−Condon theory, the excess energy may be localized on a limited number of vibrational modes immediately after the photoionization, and then be redistributed to other intramolecular modes in a femto- to picosecond time range.[55]

The temporal shift due to intermolecular vibrational relaxation has been considered to be mainly caused by anharmonic couplings with the bath of low-wavenumber modes.[48,54,57] Because of the distribution of the high excess energy, vibrational excitation of low-wavenumber modes may be substantially high after the photoionization. Consequently, the observed high-wavenumber band arises from the (0,*n*) to (1,*n*) process, where the first index refers to the vibrational quantum number of the investigated high-wavenumber mode and the second one the summation of the vibrational quantum numbers of the coupled low-wavenumber modes. Since such anharmonic coupling is expected to decrease the energy spacing between the (0,*n*) and (1,*n*) states in comparison with that between the (0,0) and (1,0) states,[54,57] the peak position of the high-wavenumber band shifts to a lower wavenumber according to the populations on the excited vibrational levels of the coupled low-wavenumber modes.

The interaction between the cation radicals and solvents is stronger than that between the neutral solutes and solvents.[58] However, the time scale of the intermolecular vibrational relaxation of the cation radicals (17 ps in acetonitrile and 13 ps in ethyl acetate in Figure 7) is roughly the same as that of the intermolecular vibrational relaxation of the polyatomic neutral molecules reported so far.[33,35,38−55,59−62] This suggests that the solute−solvent interaction has only a minor effect on the vibrational relaxation observed as the shifts of picosecond vibrational bands. This behavior can be explained by a very rapid cooling model.[39,55,59] In this model, ultrafast energy transfer from the solute to the nearest solvent shell first occurs after photoexcitation with a high excess energy, and then further heat conduction to the bulk solvent follows in tens of picoseconds. The latter picosecond process is considered to be observed as the positional changes of the picosecond Raman bands;[39] the relaxation rate of this model depends on the solvent more than the solute−solvent interaction. Intramolecular vibrational relaxation should compete with such ultrafast intermolecular energy transfer. The time constant obtained by the picosecond shift of the Raman band of *trans*-stilbene in the S_1 state was shown to have a strong correlation with the thermal diffusivity of the solvent.[39] The ultrafast intermolecular energy transfer has also been suggested from experimental[61,62] and theoretical[63] points of view. Recently, Okamoto et al. have suggested the existence of the ultrafast intermolecular energy flow in the vibrational relaxation of *trans*-stilbene in the S_1 state from picosecond time-resolved Stokes and anti-Stokes Raman spectroscopic techniques.[64]

4.2. Increases in Intensities of Cation Raman Bands on a Picosecond Time Scale. To our best knowledge, no one has reported the picosecond slow rises of cation Raman intensities after biphotonic ionization of aromatic molecules. It is unlikely that the precursor states of the cation radicals exist with lifetimes of picoseconds. This is because, as mentioned before, the ionization energies (150−162 nm) of the aromatic molecules concerned in the gas phase are much smaller than the sum of the energies of the two-pump photons (131 nm), and these ionization energies should be lowered by solute−solvent interactions. Even if the precursor state exists, internal conversion to the lowest excited state should occur on a femtosecond time scale. The intermolecular vibrational relaxation occurring on the same time scale is shown to hardly affect the resonance Raman intensities of some polyatomic neutral molecules.[26,33,48,50] Furthermore, the slow rise is not observed in ethyl acetate and 1-butanol, although the positional changes due to the intermolecular vibrational relaxation are observed in these solvents. Matousek et al. have suggested that the intramolecular vibrational relaxation process alters the Raman excitation profiles of quaterphenyl in the S_1 state, which results in the changes in the relative Raman intensities.[49] In the present study, however, no band-specific changes are observed in the cation Raman intensities within the experimental accuracy and the spectral changes are not sensitive to the probe wavelength used. Therefore, it is hard to consider that the slow increase in the cation Raman intensity in highly polar solvents is solely due to the vibrational relaxation. The dielectric relaxation time does not correlate with the rise time of the cation Raman intensity. For example, the dielectric relaxation time of acetonitrile is less than 1 ps and that of 1-butanol is about 45 ps,[20] while the slow rise is observed in acetonitrile with the time constant of 20 ps and the instantaneous rise (<5 ps) is observed in 1-butanol. Thus the rise of the cation Raman intensity is not controlled by the dielectric solvent relaxation alone. No spectral changes due to geometrical structural changes are observed in the picosecond Raman spectra of the cation radicals. From these considerations, it can be concluded that the picosecond relaxation process increasing the cation Raman intensities occurs after the photoionization of aromatic molecules.

As mentioned in subsection 4.1, immediately after the biphotonic ionization, the neighboring solvent shell of the cation radical is significantly heated by the intermolecular energy transfer process. Thus the cation radical cannot be fully solvated until the solvents are cooled through the picosecond energy flow into the bulk solvent. It is conceivable that the thermal excitation of the neighboring solvent molecules disturbs the solvation structure of the cation radical, which causes the change in the value of its electronic transition moment. As a result, the resonance Raman intensity also changes with the thermal cooling of the solvent shell. This model is consistent with the fact that the time scale of the intensity rise is the same as that of the intermolecular vibrational relaxation and the slow rise is significantly observed in highly polar solvents forming strong solvent−solute interactions. Since the electron-cation ion pair is formed immediately after the biphotonic ionization, the distance between the ions may also be changed by the intermolecular vibrational relaxation. To discuss this point more quantitatively, measurements of the probe-wavelength dependence of the Raman spectra in a much wider wavelength range are essential. The transient species in acetonitrile has been believed to be fully solvated within 1 ps by the dielectric solvent relaxation.[20] However, the present study suggests that the full stabilization of the aromatic cation radical formed by the biphotonic excitation occurs in tens of picoseconds in acetonitrile, because of the thermal excitation of the neighboring solvent shell. The importance of vibrational relaxation in the

formation of solvated aromatic ions has been suggested by Hirata et al.[65] and Oberlé et al.[26]

If the value of the electronic transition moment is changed by the disorder of the solvation structure due to the intermolecular vibrational relaxation, the slow rise may also be observed in the time-resolved electronic absorption spectra of the cation radical. Very recently we have observed femtosecond time-resolved absorption spectra of the cation radical of naphthalene, which is almost free from the overlapping with the excited-state absorption bands.[66] In acetonitrile, the rise component occurring on a 20−30 ps time scale is observed in the absorption intensity of the cation radical of naphthalene, which is consistent with the present Raman result.

5. Conclusion

Ultrafast relaxation dynamics of aromatic cation radicals following biphotonic ionization is studied by picosecond time-resolved Raman spectroscopy. In acetonitrile, Raman intensities due to the cation radicals rise in tens of picoseconds. Such a slow rise is observed in all the cation radicals treated (biphenyl, *trans*-stilbene, and naphthalene), although this behavior is not generally observed in the Raman intensities of transient neutral molecules. This result therefore indicates that the picosecond relaxation process increasing the cation Raman intensities occurs after the photoionization of aromatic molecules. No decay component is observed in all the cation Raman intensities, indicating that the geminate recombination processes do not occur in the time range of 5−200 ps. The center wavenumbers and the bandwidths of the cation Raman bands change with a time constant of 10−20 ps, which can be ascribed to the intermolecular vibrational relaxation of the cation radical toward a thermal equilibrium with solvents. The time scale of the intermolecular vibrational relaxation of the cation radicals is roughly the same as that of the intermolecular vibrational relaxation of the polyatomic neutral molecules reported, although the interaction between the cation radicals and solvents is stronger than that between the neutral solutes and solvents. This supports the ultrafast intermolecular energy flow model, in which the ultrafast energy transfer to the neighboring solvent shell first occurs and then the energy flow into outer-sphere solvent molecules follows in tens of picoseconds. The latter process determines the whole vibrational relaxation rate.

The change in the cation Raman intensity does not correlate with the dielectric relaxation time but depends on the polarity of the solvent. This indicates that the picosecond relaxation process is not controlled by the dielectric solvent relaxation alone. The time scale of the intensity rise is the same as that of the intermolecular vibrational relaxation observed as the shifts of the cation Raman bands. From these observations, we propose the model that the disorder of the solvation structure due to the intermolecular vibrational relaxation causes the change in the cation Raman intensity. It is important to emphasize that the picosecond relaxation process occurring on a 10−20 ps time scale should be taken into account for the study of photoionization of aromatic molecules.

In the time range of picoseconds, monophotonic ultraviolet ionization of the aromatic solutes is found to have negligible effects on the time-resolved Raman spectra. In the subnano- to nanosecond time range, however, contributions of the monophotonically generated cation radicals may be important as suggested by several groups.[17,21,67] Charge-pair generation, recombination, solvation and vibrational relaxation processes as well as cation structural changes can occur after photoionization of aromatic molecules in polar solvents. Solvation and intermolecular vibrational relaxation processes are discussed in the present study. The next stage of the study is to clarify the charge-pair generation and recombination processes occurring on a femtosecond time scale. Examination of intramolecular vibrational relaxation by time-resolved anti-Stokes Raman spectroscopy is also important.[48,56] The studies on the charge-pair generation and recombination processes are in progress with femtosecond time-resolved absorption measurements.[66]

Acknowledgment. This work has been supported by a Grant-in-Aid to T.N. (Grant No. 11740337) from the Ministry of Education, Science, Sports and Culture in Japan.

References and Notes

(1) Lu, H.; Long, F. H.; Eisenthal, K. B. *J. Opt. Soc. Am. B* **1990**, *7*, 1511.
(2) *The Study of Fast Processes and Transient Species by Electron Pulse Radiolysis*; Baxendale, J. H., Busi, F., Eds.; Reidel: Dordrecht, 1982.
(3) *Radiation Chemistry Principles and Applications*; Farhataziz, Rodgers, M. A. J., Eds.; VCH: New York, 1987.
(4) *Radical Ionic Systems*; Lund, A., Shiotani, M., Eds.; Kluwer: Dordrecht, 1991.
(5) Brearley, A. M.; McDonald, D. B. *Chem. Phys. Lett.* **1989**, *155*, 83.
(6) Schmidt, K. H.; Sauer, M. C., Jr.; Lu, Y.; Liu, A. *J. Phys. Chem.* **1990**, *94*, 244.
(7) Hirata, Y.; Mataga, N. *J. Phys. Chem.* **1991**, *95*, 1640.
(8) Braun, C. L.; Smirnov, S. N.; Brown, S. S.; Scott, T. W. *J. Phys. Chem.* **1991**, *95*, 5529.
(9) Sander, M. U.; Brummund, U.; Luther, K.; Troe, J. *J. Phys. Chem.* **1993**, *97*, 8378.
(10) Long, F. H.; Lu, H.; Eisenthal, K. B. *J. Phys. Chem.* **1995**, *99*, 7436.
(11) Siebbeles, L. D. A.; Emmerichs, U.; Hummel, A.; Bakker, H. J. *J. Chem. Phys.* **1997**, *107*, 9339.
(12) Onsager, L. *Phys. Rev.* **1938**, *54*, 554.
(13) (a) Hirata, Y.; Mataga, N.; Sakata, Y.; Misumi, S. *J. Phys. Chem.* **1983**, *87*, 1493. (b) Hirata, Y.; Mataga, N. *J. Phys. Chem.* **1983**, *87*, 1680. (c) Hirata, Y.; Mataga, N. *J. Phys. Chem.* **1983**, *87*, 3190. (d) Hirata, Y.; Mataga, N. *J. Phys. Chem.* **1985**, *89*, 4031.
(14) Lin, Y.; Jonah, C. D. *J. Phys. Chem.* **1993**, *97*, 295.
(15) Crowell, R. A.; Bartels, D. M. *J. Phys. Chem.* **1996**, *100*, 17940.
(16) Thomsen, C. L.; Madsen, D.; Keiding, S. R.; Thøgersen, J.; Christiansen, O. *J. Chem. Phys.* **1999**, *110*, 3453.
(17) (a) Dudev, T.; Kamisuki, T.; Akamatsu, N.; Hirose, C. *J. Phys. Chem.* **1991**, *95*, 4999. (b) Kamisuki, T.; Hirose, C. *J. Phys. Chem.* **1991**, *95*, 5003. (c) Kamisuki, T.; Dudev, T.; Hirose, C. *J. Phys. Chem.* **1991**, *95*, 5845.
(18) Maroncelli, M.; MacInnis, J.; Fleming, G. R. *Science* **1989**, *243*, 1674
(19) Barbara, P. F.; Walker, G. C.; Smith, T. P. *Science* **1992**, *256*, 975.
(20) (a) Jarzeba, W.; Walker, G. C.; Johnson, A. E.; Barbara, P. F. *Chem. Phys.* **1991**, *152*, 57. (b) Reid, P. J.; Barbara, P. F. *J. Phys. Chem.* **1995**, *99*, 3554.
(21) Sasaki, Y.; Hamaguchi, H. *J. Chem. Phys.* **1999**, *110*, 9179.
(22) Hamaguchi, H.; Gustafson, T. L. *Annu. Rev. Phys. Chem.* **1994**, *45*, 593.
(23) Vauthey, E.; Phillips, D.; Parker, A. W. *J. Phys. Chem.* **1992**, *96*, 7356.
(24) Vauthey, E.; Parker, A. W.; Nohova, B.; Phillips, D. *J. Am. Chem. Soc.* **1994**, *116*, 9182.
(25) Hub, W.; Klüter, U.; Schneider, S.; Dörr, F.; Oxman, J. D.; Lewis, F. D. *J. Phys. Chem.* **1984**, *88*, 2308.
(26) Oberlé, J.; Abraham, E.; Ivanov, A.; Jonusauskas, G.; Rullière, C. *J. Phys. Chem.* **1996**, *100*, 10179.
(27) Hofmann, M.; Zürl, R.; Graener, H. *J. Chem. Phys.* **1996**, *105*, 6141.
(28) Mizutani, Y. *J. Chem. Phys.* **1998**, *109*, 9197.
(29) Sasaki, Y.; Hamaguchi, H. *Spectrochim. Acta* **1994**, *50A*, 1475.
(30) Furuya, K.; Torii, H.; Furukawa, Y.; Tasumi, M. *J. Mol. Struct.: THEOCHEM* **1998**, *424*, 225.
(31) *CRC Handbook of Chemistry and Physics*, 81st ed.; Lide, D. R., Ed.; CRC Press: Boca Raton, FL, 2000.
(32) Reichardt, C. *Angew. Chem., Int. Ed. Engl.* **1979**, *18*, 98.
(33) Mizutani, Y.; Uesugi, Y.; Kitagawa, T. *J. Chem. Phys.* **1999**, *111*, 8950.
(34) Schneider, S.; Scharnagl, C.; Bug, R.; Baranović, G.; Meić, Z. *J. Phys. Chem.* **1992**, *96*, 9748.

(35) Weaver, W. L.; Huston, L. A.; Iwata, K.; Gustafson, T. L. *J. Phys. Chem.* **1992**, *96*, 8956.
(36) Inclusion of a Lorentzian component at ~1628 cm^{-1} is needed to reproduce the transient Raman spectrum of *trans*-stilbene in the 1560−1680 cm^{-1} region satisfactorily. The intensity of this band shows the time profile similar to those of the intensities of the S_1 bands. From ab initio molecular orbital calculations at the CIS/6-31+G* level (Sakamoto, A.; Tasumi, M., unpublished results), the 1628 cm^{-1} band may be attributed to the phenyl ring stretching mode of *trans*-stilbene in the S_1 state.
(37) Sheng, S. J.; Hug, G. *Chem. Phys. Lett.* **1978**, *57*, 168.
(38) Iwata, K.; Hamaguchi, H. *Chem. Phys. Lett*. **1992**, *196*, 462.
(39) Iwata, K.; Hamaguchi, H. *J. Phys. Chem. A* **1997**, *101*, 632.
(40) Brack, T. L.; Atkinson, G. H. *J. Phys. Chem*. **1991**, *95*, 2351.
(41) Hayashi, H.; Brack, T. L.; Noguchi, T.; Tasumi, M.; Atkinson, G. H. *J. Phys. Chem*. **1991**, *95*, 6797.
(42) Butler, R. M.; Lynn, M. A.; Gustafson, T. L. *J. Phys. Chem.* **1993**, *97*, 2609.
(43) Qian, J.; Schultz, S. L.; Bradburn, G. R.; Jean, J. M. *J. Phys. Chem*. **1993**, *97*, 10638.
(44) Hester, R. E.; Matousek, P.; Moore, J. N.; Parker, A. W.; Toner, W. T.; Towrie, M. *Chem. Phys. Lett.* **1993**, *208*, 471.
(45) Iwata, K.; Hamaguchi, H. *J. Raman Spectrosc.* **1994**, *25*, 615.
(46) Sato, S.; Kitagawa, T. *Appl. Phys. B* **1994**, *59*, 415.
(47) Qian, J.; Schultz, S. L.; Jean, J. M. *Chem. Phys. Lett.* **1995**, *233*, 9.
(48) Nakabayashi, T.; Okamoto, H.; Tasumi, M. *J. Phys. Chem. A* **1997**, *101*, 3494.
(49) Matousek, P.; Parker, A. W.; Towrie, M.; Toner, W. T. *J. Chem. Phys.* **1997**, *107*, 9807.
(50) Mizutani, Y.; Kitagawa, T. *Science* **1997**, *278*, 443.
(51) Sakai, M.; Mizuno, M.; Takahashi, H. *J. Raman Spectrosc.* **1998**, *29*, 919.
(52) Shimojima, A.; Tahara, T. *J. Phys. Chem. B* **2000**, *104*, 9288.
(53) Leonard, J. D., Jr.; Gustafson, T. L. *J. Raman Spectrosc.* **2000**, *31*, 353.
(54) Hamm, P.; Ohline, S. M.; Zinth, W. *J. Chem. Phys.* **1997**, *106*, 519.
(55) Elsaesser, T.; Kaiser, W. *Annu. Rev. Phys. Chem.* **1991**, *42*, 83.
(56) Nakabayashi, T.; Okamoto, H.; Tasumi, M. *J. Phys. Chem. A* **1998**, *102*, 9686.
(57) Asher, S. A.; Murtaugh, J. *J. Am. Chem. Soc.* **1983**, *105*, 7244.
(58) Terazima, M.; Hamaguchi, H. *J. Phys. Chem*. **1995**, *99*, 7891.
(59) Sukouwski, U.; Seilmeier, A.; Elsaesser, T.; Fisher, S. F. *J. Chem. Phys.* **1990**, *93*, 4094.
(60) Phillips, D. L.; Rodier, J.-M.; Myers, A. B. *Chem. Phys.* **1993**, *175*, 1.
(61) Okazaki, T.; Hirota, N.; Terazima, M. *J. Phys. Chem. A* **1997**, *101*, 650.
(62) Terazima, M.; Takezaki, M.; Yamaguchi, S.; Hirota, N. *J. Chem. Phys.* **1998**, *109*, 603.
(63) Nagaoka, M.; Okuno, Y.; Yamabe, T. *J. Phys. Chem*. **1994**, *98*, 12506.
(64) Okamoto, H.; Nakabayashi, T.; Tasumi, M. *J. Raman Spectrosc.* **2000**, *31*, 305.
(65) Hirata, Y.; Ichikawa, M.; Mataga, N. *J. Phys. Chem*. **1990**, *94*, 3872.
(66) Kamo, S.; Nakabayashi, T.; Sakuragi, H.; Nishi, N. Annual Review III-C-1; Institute for Molecular Science, Okazaki, Japan, 2000.
(67) Vauthey, E.; Haselbach, E.; Suppan, P. *Helv. Chim. Acta* **1987**, *70*, 347.